THE JOURNAL OF PHYSICAL CHEMISTRY B

Article

pubs.acs.org/JPCB

The −BF−NH− Link as a Peptide-Bond Surrogate

Simon Mathieu and Georges Trinquier*

Laboratoire de Chimie et Physique Quantiques (CNRS, UMR-5626), IRSAMC, Université Paul-Sabatier, 31062 Toulouse Cedex, France

ABSTRACT: A new peptidomimetic is proposed, resulting from substitution of the C═O carbonyl group by a B−F bond at the amide linkage. The effects of such chemical alteration are theoretically investigated through comparative calculations on dimethyl-fluoro-aminoborane $H_3C-BF-NH-CH_3$ and *N*-methylacetamide $H_3C-CO-NH-CH_3$, the simplest model of a peptide linkage. While little difference is found regarding size, electronic structure, and plaque rigidity, substantial distinctions are, however, observed between the polarities and association energies of the two compounds, with a B−F···H−N hydrogen bond estimated to be about one-third as strong as the natural C═O···H−N one. The conformational maps of the corresponding dipeptide models exhibit similarities and distinctions, which partly account for helical oligomer properties. Although capable of a high level of organization, the chains made of fluoro-aminoborane units show overall less structuration and more plasticity than their peptidic counterparts. Contrasts with fluorine-containing peptidomimetic 2-fluoro-2-butene are further underlined.

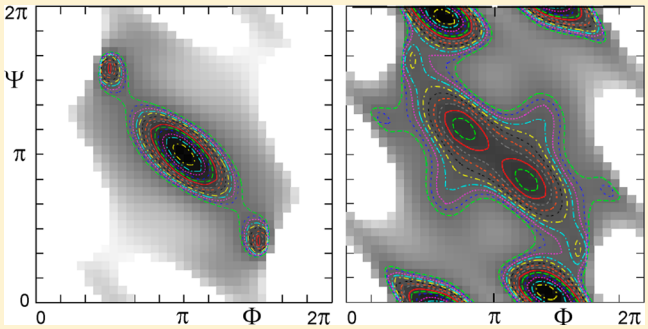

INTRODUCTION

Peptides are an important class of molecules involved in many biological processes. Their low biostability, in particular toward proteolytic cleavage of the amide linkage, however, limits their use as therapeutic agents in medicinal applications. Attempts to build peptide-like compounds with enhanced stability or pharmaceutical potentials have contributed to the development of peptidomimetics.[1−10] Focusing on modifications to backbone and/or side chains of single or multiple peptide fragments, biomimetic strategies have provided various classes of peptidomimetic compounds. In particular, the replacement of the −CO−NH− amide bond, the main site of peptide degradation, by fluoroalkenes has been widely experimented as the amide-bond geometrical features are rather well-reproduced by a planar olefinic moiety.[11−19]

The fluorobutene sequential unit $-CH_2-CF{=}CH-CH_2-$ actually mimics the main features of the elementary peptidic plaque $-CH_2-CO-NH-CH_2-$. Both molecular frameworks are similar in (i) the number of atoms and their arrangement, (ii) the skeleton planarity, and (iii) bond polarizations, as highly electronegative fluorine mimics carbonyl oxygen to some extent. The elementary structural unit of fluoroalkene, the 2-fluoro-2-butene (2FB) $H_3C-CF{=}CH-CH_3$ has been theoretically investigated[14,19] as a promising isostere of the simplest model of peptide linkage in proteins, namely, *N*-methylacetamide (NMA) $H_3C-CO-NH-CH_3$. If both compounds are found to be structurally similar, there are two substantial differences: fluorine is a weaker hydrogen-bond acceptor than carbonyl oxygen, and the olefinic C−H bond in the fluoroalkene, although carrying a somewhat acidic hydrogen, is of course much less inclined to hydrogen bonding than is peptidic N−H. Another noticeable difference stems from the rigidity of the olefinic moiety with respect to the rather flexible ω backbone torsion angle around the amide bond.[20] These two drawbacks obviously disfavor fluoroalkenes in partaking in interactions suited for secondary and tertiary structures of proteins.

Aside from fluoroalkenes, organoboranes have also been considered as potential peptide substitutes. Aminoboranes, for instance, present both good hydrocarbon isosterism[21] and interesting pharmacological properties.[22] According to theoretical studies of boron substitution at either Cα, C′, or N peptidic sites,[23−27] and in contrast to fluoroalkenes, boron isosteres present more realistic flexibility around the pseudo amide bond, even if they do not attain the right peptide rigidity.

As a further step in the pursuit of closer similarity with the amide linkage, we report in the present work a simple combination of fluoroalkene and organoborane favorable features. The replacement of the carbonyl group by the BF bond in NMA leads to dimethyl-fluoro-aminoborane (DFA) $CH_3-BF-NH-CH_3$. Since the C═O and B−F bonds have the same length and the same number of electrons, the atoms in DFA are expected to serve as a satisfactory topographical mimic. The high polarity of the B−F bond is further expected to enhance the hydrogen-bond acceptor character of fluorine, with respect to that observed in simple fluoroalkenes. Last, the torsional ease around the pseudo peptide bond B−N is also expected to reflect that in peptides, as shown on amino-

Received: April 30, 2012
Revised: June 21, 2012
Published: July 13, 2012

dx.doi.org/10.1021/jp304150p | *J. Phys. Chem. B* 2012, 116, 8863−8872

boranes.[28] Size, polarization, flexibility, the ability to hydrogen bond, and the ingredients underpinning the propensity to form secondary structures will therefore be theoretically described in this order for DFA, NMA, and 2FB for the sake of comparison. Next, dipeptide-model conformational maps, *trans*-plaque association, and helical oligomers will be addressed for DFA and NMA.

COMPUTATIONAL DETAILS

All calculations were carried out with the Gaussian03 quantum chemistry package, at the DFT-B3LYP and MP2 levels of theory, using the 6-311G** basis set.[29] Complete geometry optimizations were done at both DFT and MP2 levels, with energy gradients lower than 10^{-6} au, except for some dipeptide -model dimers and all helical oligomers, where gradients of only 10^{-4} au could be reached. All stationary points were characterized as true minima or transition states on the potential energy surface by calculating the corresponding harmonic vibrational frequencies, except for dipeptide-model dimers and helical oligomers. For interaction energies in dimer complexes, basis set superposition errors (BSSE) were estimated by the standard counterpoise procedure. The rotational barrier in 2-fluoro-2-butene was evaluated at the multiconfigurational level through a CASSCF(2,2) procedure. The Ramachandran maps of the dipeptide models were calculated using frozen geometries corresponding to those optimized at the β-zone extended conformation. Each dihedral angle Φ and Ψ is varied in steps of 10°. Because of the symmetry, only half of the 1296 points covering the full map need to be calculated.

RESULTS AND DISCUSSION

Structural Features. Even though NMA and 2FB have been previously described by means of accurate calculations,[14,30−32] the geometries of the three kinds of plaques have been optimized here for the sake of consistency. The main geometrical parameters are gathered in Table 1. There is little difference between DFT and MP2 values, except the slight departure from planarity of *trans*-*N*-methylacetamide revealed at the MP2 level. As for the two fluorinated isosteres, *cis*- and *trans*-structures are encountered to be rigorously planar, regardless of the level of description. Unless otherwise mentioned, the discussion below will refer to the geometrical parameters obtained for the *trans*-rotamers. In Figure 1, the NMA, 2FB, and DFA plaques are drawn to the same scale, together with their dipole moments. At first sight, the three frameworks have roughly the same shape and the same size. There is, however, a blindingly obvious difference in the magnitudes of dipole moments. Their values, 4.0 D for NMA, 1.7 D for 2FB, and 2.3 D for DFA, highlight the deficiency of both mimicking isosteres, especially the fluorobutene, to reflect electric properties of a natural peptide.[33] Nevertheless, the dipole-moment *orientations* of our models are not that bad, particularly that of aminoborane. The global trapezoid shape of NMA, circumscribed by the dotted line in Figure 1, is also better reflected by that of DFA, whereas fluorobutene is instead inscribed in a parallelogram. Comparison of the overall dimensions of the plaques can be given by the $C_1\cdots C_4$ distances separating the two α carbons. As diagonals of the *trans*-plaques, they echo the length of the elemental links in a peptide chain. This parameter is slightly larger in both mimicking plaques than in the parent amide, by 5% and 10%

Table 1. Summary of Plaque Geometrical Parameters[a]

		DFT		MP2	
		trans	*cis*	*trans*	*cis*
N-methyl acetamide	C1−C′	1.521	1.520	1.519	1.518
	C′−N	1.367	1.371	1.369	1.376
	N−C4	1.453	1.453	1.451	1.452
	C═O	1.219	1.218	1.222	1.221
	N−C═O	123.1	121.3	122.8	121.6
	C1C′NC4 (ω)	180.0	7.3	173.7	17.8
	OC′NH	180.0	−4.1	−170.4	−9.6
	C1···C4	3.819	2.937	3.800	2.903
	μ	3.69	3.97	4.03	4.29
2-fluoro 2-butene	C1−C	1.489	1.490	1.490	1.491
	C═C	1.327	1.328	1.336	1.336
	C−C4	1.499	1.500	1.500	1.500
	C−F	1.368	1.368	1.359	1.360
	C═C−F	119.6	118.0	120.0	118.3
	C1···C4	3.934	3.208	3.932	3.193
	μ	1.45	1.77	1.69	2.04
dimethyl fluoro aminoborane	C1−B	1.571	1.570	1.574	1.573
	B−N	1.398	1.399	1.400	1.400
	N−C4	1.457	1.453	1.456	1.452
	B−F	1.359	1.361	1.356	1.359
	N−B−F	117.6	115.5	118.0	116.1
	C1···C4	4.000	3.264	3.994	3.244
	μ	2.24	2.30	2.26	2.37

[a]Bond lengths in Angströms, angles in degrees, and dipole moments in Debyes.

for *trans*- and *cis*-forms, respectively, with an effect more marked in the aminoborane (see Table 1).

Bonding. The π system in amides is generally described by resonance forms, giving the CN bond its partial double-bond character and conferring on the CO bond a less-than-double character, thereby intensifying its polarity $O^--{}^+C$.[34,35] The resulting peptide backbone is thus maintained planar, with slight fluctuations of the central-bond torsional angle around $\omega \approx 180°$.[20] Similar resonance forms can be drawn in DFA (cf. Scheme 1), suggesting common features for B−N and C−N bonds, and a π polarity formally different for F−B and O−C, an effect overcompensated in the σ system by the strong electronegativity of fluorine. It is convenient to portray such π systems as three-center, four-electron (3c−4e) bonds, also called electron-rich bonds. This concept, proposed long ago in different contexts,[36,37] is well suited to summarize the π organization in peptidomimetic candidates. In peptide bonds, the four electrons stem from the carbonyl π bond and from the $2p_z$ nitrogen lone pair. Similarly, the three-orbital interaction in fluoroaminoborane occurs between full 2p(F), vacant 2p(B), and full 2p(N) valence orbitals. The provenance of the four π electrons in NMA, DFA, and 2FB therefore corresponds to 1−1−2, 2−0−2, and 2−1−1 schemes, respectively. This initial partition is next adjusted by delocalization effects, the extent of which can be assessed from the calculated π populations. These are reported in Table 2, together with the corresponding π and

dx.doi.org/10.1021/jp304150p | J. Phys. Chem. B 2012, 116, 8863−8872

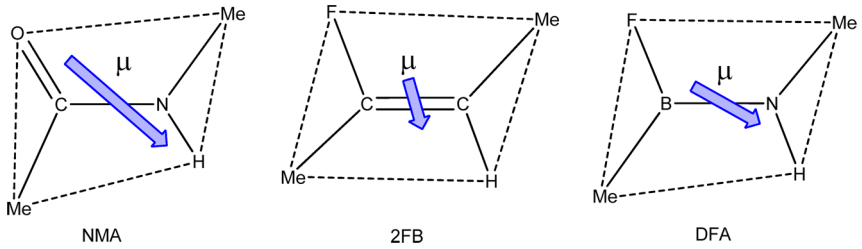

Figure 1. Comparative sizes of *trans*-plaque for *N*-methylacetamide (NMA), 2-fluoro 2-butene (2FB), and dimethyl-fluoro aminoborane (DFA), with corresponding dipole moment orientations and relative magnitudes, calculated at the DFT level.

Scheme 1

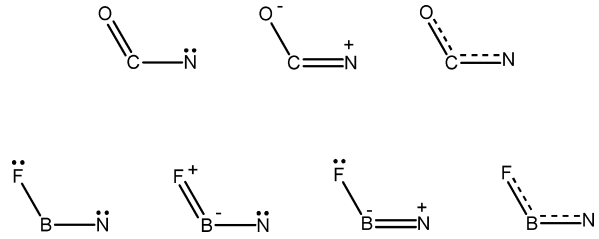

global ($\sigma + \pi$) net charges. A fourth compound, planar-constrained dimethyl-vinylamine $CH_3-C(CH_2)-NH-CH_3$, is included here in the set for the sake of comparison. By comparing the lines "π initial" and "π population", one first sees the (3c–4e) bonding at work, tending to restore electron preeminence at the ends of the frame. This occurs of course to a different extent, depending on the initial allocation and on the nature of each atom. The lines "π net charge" bring out the contrast in π polarity between NMA and its substitutes, especially DFA. When σ electrons are taken into account (cf. lines "whole ($\sigma + \pi$)"), σ-inductive effects and electronegativity restore in all cases a polarity more in line with that of NMA, and again DFA does a little better than its contenders.

Plaque Rigidity and Flexibility. Molecular electronic levels corresponding to the higher occupied and lower unoccupied orbitals of DFA are depicted together with those of NMA in Figure 2. The π-level splitting (red lines) suggests stronger orbital interaction in DFA. Since π_2 electrons are basically nonbonding, while π_1 electrons strengthen the three-center bond, the lower π_1 level in aminoborane should confer a little more rigidity upon rotation around B–N, when compared to that around C′–N in peptides. Given the low electronegativity of boron, the charge separation along the BF and BN bonds is substantial. The resulting electrostatic attraction may contribute to a BN bond length of 1.40 Å, quite in line with that of formally double BN bonds.[38]

By contrast, the central bond in fluoroalkene is better seen as a plain double bond, with two-center, two-electron π interaction. Indeed, the CC bond length of 1.34 Å calculated in 2FB is typical of that commonly encountered in alkenes. The resulting rigidity of fluoroalkene may be expected to be detrimental to the rotational partial freedom and should therefore dramatically interfere in the protein folding. Not only peptide bonds reveal significant departures from planarity in peptides and proteins[20] but also ω torsion angles were shown to be correlated to the adjacent ψ angle.[39]

The *trans* versus *cis* conformational preference of the amide bond is known to be around 2.5 kcal/mol with a rotational barrier of about 19 kcal/mol to overcome from the *trans*-form. The structural preference is less marked in the mimicking

Table 2. Mulliken π Populations on the Three Centers of the (3c–4e) Bonds in *trans*-NMA Analogues, Calculated at the DFT Level

	3c atoms		X	C′	N	Σ
Me–CO–NH–Me (*trans*-NMA)	O–C–N	π initial	1	1	2	4
		π population	1.44	0.87	1.68	3.99
		π net charge	−0.44	+0.13	+0.32	0
		whole ($\sigma + \pi$)	−0.38	+0.31	−0.41	0
Me–BF–NH–Me (*trans*-DFA)	F–B–N	π initial	2	0	2	4
		π population	1.85	0.50	1.65	4.00
		π net charge	+0.15	−0.50	+0.35	0
		whole ($\sigma + \pi$)	−0.23	+0.42	−0.40	0
Me–CF=CH–Me (*trans*-2FB)	F–C–C	π initial	2	1	1	4
		π population	1.90	1.04	1.09	4.02
		π net charge	+0.10	−0.04	−0.09	0
		whole ($\sigma + \pi$)	−0.25	+0.19	−0.22	0
Me–C(=CH2)–NH–Me (*trans*)[a]	C–C–N	π initial	1	1	2	4
		π population	1.21	0.98	1.72	3.91
		π net charge	−0.21	+0.02	+0.28	0
		whole ($\sigma + \pi$)	−0.31	+0.13	−0.44	0

[a]With planarity constraint (1*i*).

dx.doi.org/10.1021/jp304150p | *J. Phys. Chem. B* 2012, 116, 8863–8872

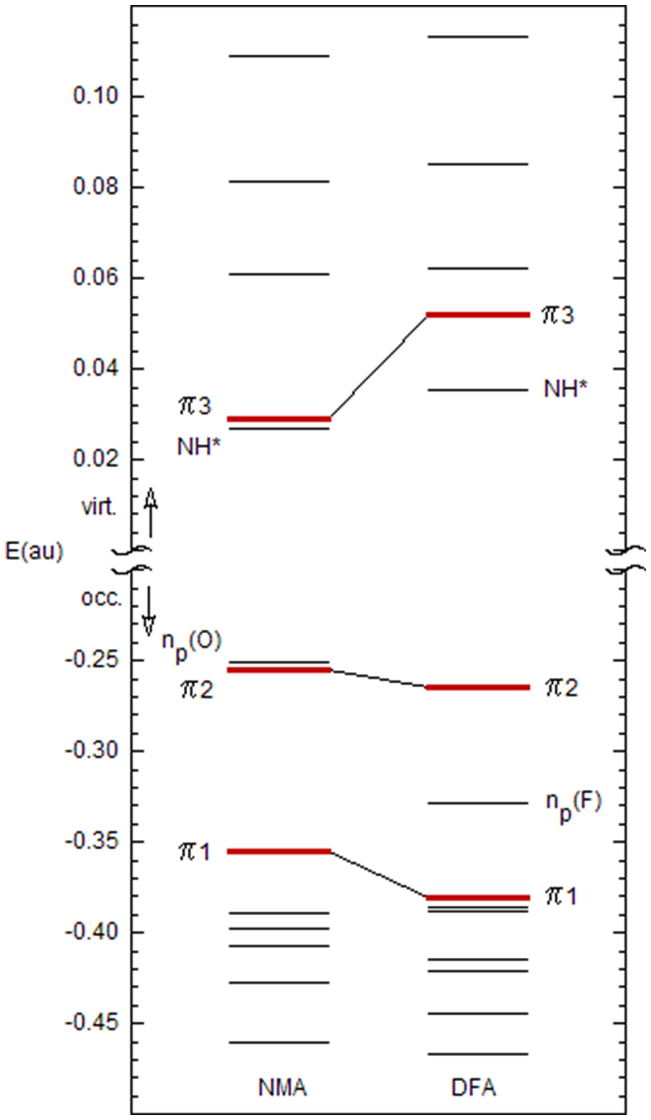

Figure 2. Orbital level diagram for *trans*-NMA and *trans*-DFA, highlighting the π-allyl set.

compounds, especially in DFA, where this difference reduces to 0.8 kcal/mol (see Table 3). It is arguable to what extent steric constraints in the *cis* form, where methyl groups are on the same side of the central bond, increase as the overall size of the plaque decreases, going from DFA to NMA. Thinking of forward consequences in oligomer structures, one will keep in mind that such *cis* steric obstruction can be partially relieved through proper adjustment of the backbone dihedral angles, including torsional ω.[40]

Owing to the nature and strength of the π bonding in these systems, the heights of the barrier to rotation are ordered as follows: NMA $\leq$ DFA $\ll$ 2FB, as reported in Table 3. The barriers in NMA and DFA are quite comparable, around 20 kcal/mol. Of course, that in 2FB reflects that of an ethylenic double bond around 70 kcal/mol.[41] For the analogous cases of NMA and DFA, two rotational paths via nonequivalent transition structures were found, with opposite pyramidalization of the amine group. As documented on NMA,[30] the lowest energy transition state TS1, exhibits an "up" form with both substituents at N bent toward the CO (BF) bond, while TS2 has a "down" form with opposite pyramidalization of the amine

Table 3. Summary of Plaque Energetics (in kcal/mol) for *N*-Methylacetamide (NMA), 2-Fluoro 2-Butene (2FB), and Dimethyl-Fluoro Aminoborane (DFA)[a]

			ΔE	ΔE + ZPE	ΔG^0_{298}
DFT	NMA	TS2	22.2	21.5	22.5
		TS1	18.4	17.9	19.1
		cis	2.7	2.6	2.8
		trans	0.0	0.0	0.0
	2FB	TS2[b]	67.1		
		TS1[b]	66.8		
		cis	1.7	1.7	1.6
		trans	0.0	0.0	0.0
	DFA	TS2	24.3	23.0	23.0
		TS1	23.4	22.1	22.3
		cis	0.8	0.8	0.5
		trans	0.0	0.0	0.0
MP2	NMA	TS2	19.7	19.3	20.8
		TS1	15.7	15.5	17.1
		cis	2.2	2.5	3.6
		trans	0.0	0.0	0.0
	2FB	*cis*	1.8	1.7	1.6
		trans	0.0	0.0	0.0
	DFA	TS2	23.8	22.6	22.6
		TS1	22.8	21.7	22.0
		cis	0.8	0.7	0.4
		trans	0.0	0.0	0.0

[a]ZPE stands for zero-point vibrational energies. [b]Determined at the CASSCF(2,2) level.

group. TS1 is therefore geometrically closer to the *trans*-form, while TS2 is closer to the *cis* one (see the ω torsion angles in Table 4). Two transition structures have also been located through the CASSCF(2,2) procedure for fluorobutene. In this case, the transition states are quasi degenerate with nearly the same geometrical parameters, only differing in "backbone" dihedral angles, TS1 being here again closer to the *trans*-structure and TS2 closer to the *cis* one.[42] Given the complex nature of the *cis*−*trans* isomerization, a complete description of the whole rotational process is beyond the scope of the present work, which only addresses comparisons of energetics for the three isosteres under scrutiny. This short analysis of internal rotations underlines how fluorobutene exhibits much less intraplaque flexibility than the other two isosteres.

Hydrogen Bonding. As previously proposed in a study of hydrogen-bond relative strengths,[43] we can take advantage of the arrangement of *cis*-plaques to construct stables dimers. Since the complexes formed in this way (see Scheme 2) happen to be true minima on the corresponding potential energy surfaces, constraint-free optimizations can be carried out. Not surprisingly, the optimized values of X−H···Y valence angle border on 180° in all three dimers (see Table 5).[44] Among the low-frequency harmonic vibrational modes of the dimers, a rather pure one corresponds to the joint stretching of the two equivalent XH···Y bonds, each monomer staying relatively rigid, from which the hydrogen-bond stretching force constants can be determined.[45] Gathered in Table 5, geometries, force constants, and binding energies all suggest that the hydrogen

dx.doi.org/10.1021/jp304150p | J. Phys. Chem. B 2012, 116, 8863−8872

Table 4. Selected Geometrical Parameters (Å and deg) for the Transition States Connecting the *cis*- and *trans*-Isomers of *N*-Methylacetamide (NMA) and Dimethyl-Fluoro-Aminoborane (DFA)

		DFT		MP2	
		TS1	TS2	TS1	TS2
NMA	C′−N	1.457	1.451	1.455	1.449
	C═O	1.204	1.201	1.211	1.208
	N−C═O	122.9	120.4	123.1	120.6
	C′−N−H	105.9	108.6	105.2	107.2
	CCNC (ω)	122.7	59.1	124.0	56.7
	OCNH	59.8	115.1	59.7	118.2
	Σ C′	360.0	360.0	360.0	360.0
	Σ N	325.4	333.4	318.2	328.2
DFA	B−N	1.460	1.460	1.465	1.465
	B−F	1.351	1.342	1.347	1.338
	N−B−F	118.9	116.9	119.2	117.3
	B−N−H	110.9	111.6	109.4	110.0
	CBNC (ω)	117.5	64.3	119.6	62.0
	FBNH	63.0	116.4	61.2	118.9
	Σ B	360.0	360.0	360.0	360.0
	Σ N	335.8	337.7	330.5	332.4
2FB	C−C	1.477	1.478		
	C−F	1.352	1.353		
	C−C−F	112.9	112.8		
	C−C−H	116.7	117.3		
	CCCC (ω)	133.0	71.7		
	FCCH	68.0	89.5		
	Σ C(F)	355.8	355.7		
	Σ C(H)	347.1	347.3		

Scheme 2

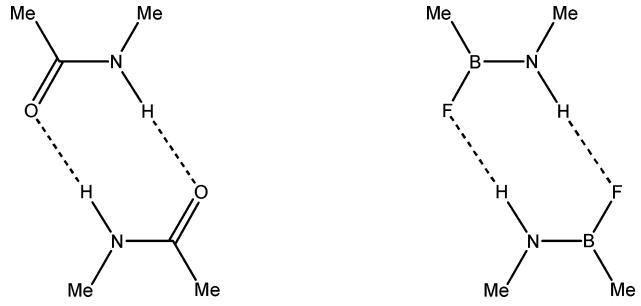

bonding in aminoborane is here between half and third as strong as in NMA, still in the range of organic XH···Y hydrogen bonds. By contrast, only a tiny interaction seems to link two fluorobutenes at this level of description.

From overall comparisons of monomers, it is clear that fluoro-aminoborane mimics natural peptides better than does fluoro-butene. Though the three-dimensional structure of the latter is close to that of a *trans*-peptide frame, especially in the C$\alpha(i)$···C$\alpha(i+1)$ distance, both plaque rigidity and poor hydrogen-bonding capability make fluoroalkenes unsuitable for secondary structures. By contrast, in DFA, the simple substitution of CO by BF allows most of the properties of the peptide bond to be preserved to some extent.

Table 5. Calculated Intermolecular and Hydrogen-Bond Parameters for *cis* Dimers[a]

		$d_{H\cdots O/F}$	$\theta_{X-H\cdots O/F}$	$\bar{\nu}_{H\cdots O/F}$	$k_{H\cdots O/F}$	1/2 ΔE_{dim}	1/2 ΔE_{dim} (CP)
DFT	NMA	1.86	180	150	0.24	−8.0	−6.4
	DFA	2.08	173	92	0.09	−3.2	−2.4
	2FB	2.47	178	56	0.03	−1.3	−0.3
MP2	NMA	1.86	179	141	0.22	−8.0	−5.7
	DFA	2.08	174	93	0.09	−3.5	−2.3
	2FB	2.46	176			−1.7	−0.6

[a]Bond lengths in Å, angles in degrees, wavenumbers in cm^{-1}, force constants in mdyn/Å, and energies in kcal/mol. CP stands for counterpoise correction.

Dipeptide Models. As a step further in the study of similarity to peptide, one must be concerned with the properties of *successions* of plaques; in other words, one would like to compare a polymer made of our aminoborane units with a plain polypeptide chain. This calls for the knowledge of the allowed conformations that are induced by favorable combinations of (Φ/Ψ) sets along the backbone. We are thus led to the study of dipeptide models made of our plaques, namely, the glycine dipeptide $CH_3-CO-NH-CH_2-CO-NH-CH_3$ and its BF analogue $CH_3-BF-NH-CH_2-BF-NH-CH_3$. As a preliminary test of stability, we first evaluate the *plaque junction energy* (PJE), which measures the ease to build polypeptide chains from isolated plaques.[46] In our case, it is defined by the energy of the isodesmic reactions:

$$2\ CH_3-CO-NH-CH_3 \rightarrow CH_3-CO-NH-CH_2-CO-NH-CH_3 + CH_4$$

$$2\ CH_3-BF-NH-CH_3 \rightarrow CH_3-BF-NH-CH_2-BF-NH-CH_3 + CH_4$$

the dipeptide being taken in its non-γ best minimum in order to prevent specious intramolecular hydrogen bonding. With a weak negative PJE around −0.8 kcal/mol, DFA does not favor such a coupling as much as NMA does, with an increment around −5 kcal/mol (see Table 6).

The Ramachandran conformational maps for the all-*trans* forms of both dipeptide models have been calculated at the DFT level and are shown in Figure 3. Since the Cα are nonsubstituted, as in glycine, the maps exhibit a 2-fold rotation symmetry. As a consequence, to each (Φ/Ψ) set of dihedral angles, hereafter expressed in degrees, will correspond a symmetrical companion, in which the angles have opposite values.

At our level of description, the glycine dipeptide has two catchment regions here (Figure 3, top). The lower one is centered in the extended β zone, corresponding to β-strand arrangements, around (−180/180). The second one is centered in the γ-turn zone, around (−80/70).[47] According to the map, the latter conformation lies about 1 kcal/mol above the former, with a barrier of about 2.7 kcal/mol to their interconversion, near (−110/110). In an isolated dipeptide, this γ-turn region is artificially stabilized by intra-dipeptide hydrogen bonding between the farthest CO and NH groups. Because full geometry optimization in this region makes possible a fine-tuning of the hydrogen-bond geometry, the γ-form is actually calculated to lie about 1 kcal/mol *below* that of the optimized β-form (see Table 6, left). A reverse effect applies in the α-helix region, around (−60/−40), where no extra-dipeptide hydrogen bonding is possible here, in contrast to widespread helicolidal

dx.doi.org/10.1021/jp304150p | J. Phys. Chem. B 2012, 116, 8863−8872

Table 6. Summary of Results for the Dipeptide Models Built from *trans*-NMA and -DFA Plaques[a]

		NMA		DFA	
parameter	minimum	DFT	MP2	DFT	MP2
(Φ/Ψ)	β	(180/180)	(−175/−166)	(−137/145)	(−133/139)
	γ	(−82/70)	(−81/80)	(−78/64)	(−81/79)
	δ			(−119/10)	(−117/10)
$d_{H\cdots X}$	γ	2.07	2.07	2.26	2.41
$\theta_{N-H\cdots X}$	γ	144	143	138	129
PJE[b]	β	−4.4	−5.5	−0.4	−1.3
ΔE	β	0.8	1.8	1.0	1.5
	γ	0	0	1.8	1.7
	δ			0	0

[a]Bond lengths in Angströms, angles in degrees, and energies in kcal/mol. [b]Plaque junction energy (see text for the definition).

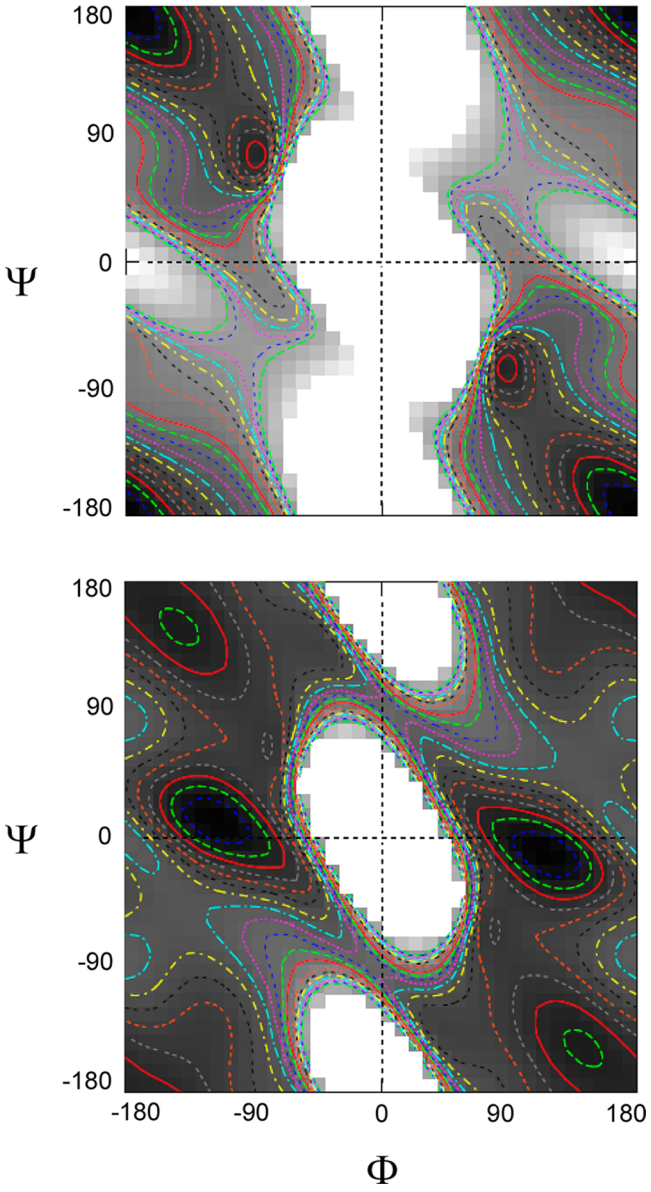

Figure 3. DFT-calculated Ramachandran maps for *trans*-dipeptide models of NMA (top) and DFA (bottom). Contour lines run from 0.5 to 10 kcal/mol with regular steps of 0.5 kcal/mol. Gray shading rises up to 20 kcal/mol.

polymers.[48,49] Nevertheless, this region forms a clear plateau lying at 3−4 kcal/mol above the extended minimum.

The map of the DFA dipeptide displays notable differences (Figure 3, bottom). The absolute minimum is now located in a large basin around (−115/15), close to the δ-zone.[50] The β-region is still a clear catchment region, around (−140/150), lying about 1 kcal/mol higher. The γ-turn region is now reduced to a narrow shallow secondary minimum, around (−65/80), at about 2 kcal/mol above the absolute minimum. Notice a fourth local minimum in highlands at 4 kcal/mol, around (−180/85), which could also be affiliated to the δ region. Interconversion between the δ and β forms should require a barrier of 2−2.5 kcal/mol above the former, while that between the β and γ forms should require a barrier of 1.5 kcal/mol above the former. As on the glycine map, the α-helix region also corresponds here to a clear plateau, lying 3−4 kcal/mol above the δ region, and directly accessible from it. The optimized geometrical parameters and relative energies of the three main minima are reported in Table 6, right. A characteristic of the δ conformation is that the dihedral angle between the two plaques is close to 120°. This type of conformation is also found to be a stable form of the *trans*-dipeptide model constructed from 2FB plaques, namely, $CH_3-CF{=}CH-CH_2-CF{=}CH-CH_3$, the (Φ/Ψ) sets being calculated at (−119/11) and (−117/10) at the DFT and MP2 levels, respectively.

Exploration of isolated dipeptide models clearly suggests more conformational accessibility in DFA, as illustrated by drawing the corresponding maps along noncanonical intervals of [0−360°] for Φ and Ψ. This representation shows how the (Φ = 0) zone is no longer forbidden in DFA, where the two symmetrical regions can be linked through a barrier of 4−4.5 kcal/mol near (−10/−90). We next examine how such dipeptide models can associate into hydrogen-bonded systems through *trans*-plaque connections, like those occurring in real secondary and tertiary structures.

***trans*-Plaque Association.** Formally, dipeptide-model dimers can be seen as elementary structural units of antiparallel β sheets. Two pairing schemes are possible, labeled from the size of the ring created by the double binding. In the S14 layout, the hydrogen bonds involve extreme NH and CO groups, while, in the S10 layout, they involve the middle ones (Scheme 3). S14 corresponds to extended backbones, while, in fact, S10 corresponds to γ-turn ones, preserving additional intrastrand hydrogen bonds and in no way reflecting β-sheet structure. On the other hand, it is clear that the δ-forms of DFA dipeptides do not allow straightforward association. The calculated geometries and energies for both arrangements are summarized in Table 7. From the (Φ/Ψ) sets, little backbone deformation occurs upon pairing. The h10 hydrogen-bond *d*

dx.doi.org/10.1021/jp304150p | J. Phys. Chem. B 2012, 116, 8863−8872

Scheme 3

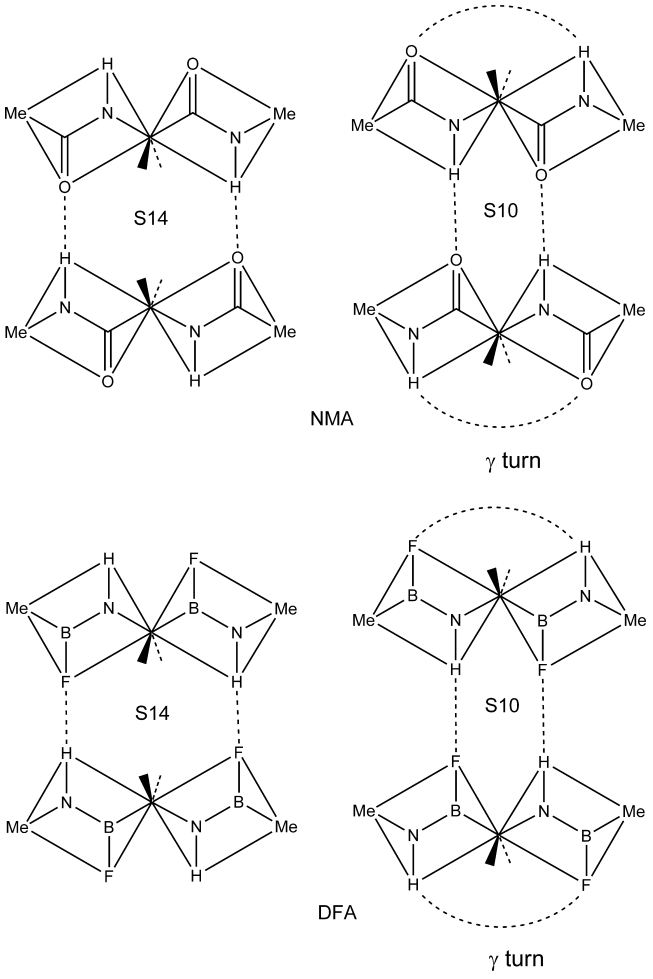

and θ parameters are close to those discussed above for *cis*-plaques dimers, again implying a C═O···H interaction stronger than the B−F···H one. When reduced to hydrogen-bond elemental increments, the relative energies lead to comparable BF···H interactions in dimers built from *cis*-plaques or *trans*-dipeptides (namely, 2 kcal/mol, cf. Tables 5 and 7). This is not the case for NMA CO···H interactions, which are significantly higher in the *trans*-dipeptide dimers than in the *cis*-plaque dimer, (8 vs 6 kcal/mol, cf Tables 5 and 7), indicative of large global interactions in the former. Since the contrast is more patent at the MP2 level, its origin could lie in dispersion effects between the two facing backbones. Defining local hydrogen-bond increments may therefore not be well-founded in this case.

Helical Oligomers. Further single-strand structuration has been examined by exploring two kinds of helices. In the first one, each Cα is assigned the environment corresponding to the δ-zone in the dipeptide map discussed above. Optimization at the DFT level of such an arrangement of 20 DFA *trans*-plaques (19 Cα) led to a regular helix with all (Φ/Ψ) sets keeping close to the δ-assignment ((−105/8) vs (−119/10), see Tables 6 and 8). The regularity of this helix is conspicuous from Figure 4, top, and from the standard deviations of dihedral angles, given in Table 8. It originates in (i) the sturdy character of the δ catchment region in the dipeptide map and (ii) the

Table 8. Summary of DFT-Calculated Structural Results for Some Helical Oligomers of Various Sizes[a]

			(Φ/Ψ)		
plaque	type	N(Cα)	mean	SD	MPJE
DFA	δ	19	(−105/8)	(4/01)	−0.5
DFA	α	13	(−87/-24)	(21/16)	−0.5
NMA	α	13	(−73/-33)	(18/13)	−6.0
2FB	δ	18	(−113/9)	(2/01)	−0.2

[a]Angles in degrees; MPJE in kcal/mol (see text for the definition).

Table 7. Summary of Intermolecular and Intramolecular Parameters for All-*trans* Dipeptide-Model Dimers[a]

			NMA		DFA	
pairing	parameter		DFT	MP2	DFT	MP2
S10	$d_{H\cdots Y}$	h10	1.87	1.85	2.12	2.09
	$\theta_{X-H\cdots Y}$	h10	170	171	159	159
	$d_{H\cdots Y}$	h7	2.00	1.97	2.25	2.24
	$\theta_{X-H\cdots Y}$	h7	144	144	136	134
	(Φ/Ψ)		(−81/77)	(−81/80)	(−77/70)	(−77/72)
	1/2 ΔE_{dim}		−9.5	−11.0	−3.2	−4.1
	1/2 ΔE_{dim} (CP)		−7.5	−7.8	−1.8	−2.3
S14	$d_{H\cdots O/F}$		1.95	1.93	2.09	2.08
	$\theta_{X-H\cdots O/F}$		166	165	164	163
	(Φ/Ψ)		(−175/174)	(−178/174)	(131/-139)	(132/-138)
	1/2 ΔE_{dim}		−9.0	−11.0	−4.2	−5.1
	1/2 ΔE_{dim} (CP)		−7.1	−8.2	−2.0	−2.2

[a]Bond lengths in Angströms, angles in degrees, and energies in kcal/mol. For S10 arrangements, h10 and h7 refer to the intermolecular and intramolecular hydrogen bonds, respectively. ΔE_{dim} refer to separated dipeptides optimized in their closer minimum. CP stands for counterpoise correction.

dx.doi.org/10.1021/jp304150p | J. Phys. Chem. B 2012, 116, 8863−8872

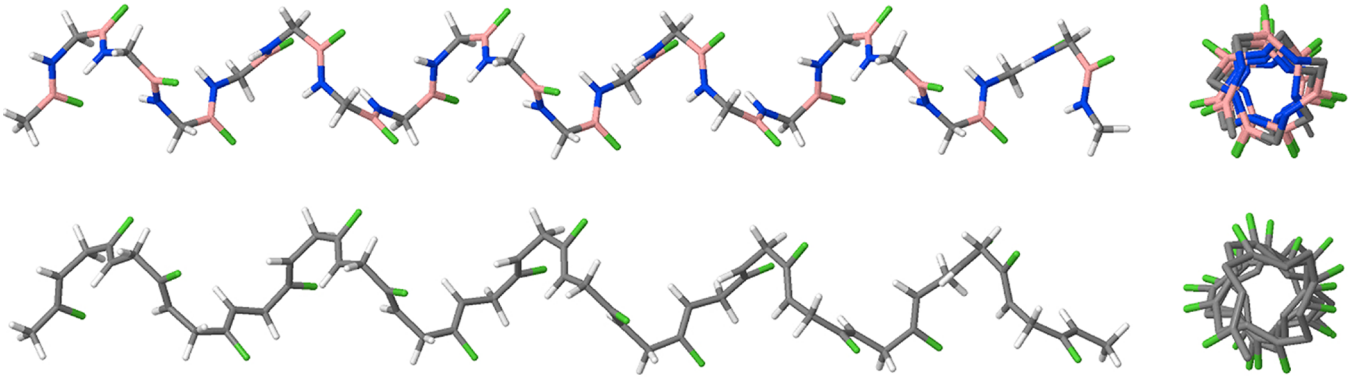

Figure 4. DFT-optimized δ-type helices obtained from 20 plaques of DFA (top) and 19 plaques of 2FB (bottom).

impossibility of intramolecular hydrogen bonding in this conformation, which explains the absence of end effects and reinforces the regularity. As the 2FB dipeptide map also exhibits a marked δ-zone, the same causes leading to the same effects, a similar structure is expected to be stable for a helix of fluorobutene plaques. In fact, an optimized δ-type helix made of 19 2BF plaques (18 Cα) contains the same structural features as that of DFA (see Figure 4, bottom, and Table 8). The mean (Φ/Ψ) set is here around (−113/9) (vs (−119/11) in the dipeptide), with again small standard deviations around these values. Not unexpectedly, the same type of helix is also observed in chains of the simply olefinic 2-butene plaques (when double bonds are in *cis* configuration, this corresponds to the polyunsaturated fatty chains encountered in natural lipids).[51]

The structures of these oligomers make it possible to estimate the helical parameters of the δ-helix. For DFA, the pitch is measured at about 7.8 Å, and the rise at about 103°, corresponding to 3.5 residues per turn. For the 2FB helix, these parameters are 8.6 Å, 96°, and 3.7 residues per turn. These numbers point to structures that are significantly more stretched than classical α-helices.

As a stability indicator, we can use the PJE increment defined above, now averaged over all n junctional Cα's, thus defining a *mean plaque junction energy* (MPJE). This convenient normalized index is given straightforwardly by the equation

$$\mathrm{MPJE} = \frac{1}{n}E_{\mathrm{helix}} + E_{\mathrm{methane}} - \frac{n+1}{n}E_{\mathrm{plaque}}$$

where the E terms refer to total energies of helix, CH_4, and elemental plaque $CH_3{-}BF{-}NH{-}CH_3$ (or $CH_3{-}CF{=}CH{-}CH_3$), respectively. For the δ-helical oligomers, this index is calculated at −0.5 kcal/mol for DFA and −0.2 kcal/mol for 2FB.

We next inspect the possibility of intramolecular hydrogen bonding in α-helices. Oligomers of 14 NMA and DFA plaques (13 Cα) were optimized, starting from a regular geometry with all Cα assigned to ideal α-helix environments. Hydrogen bond-structured helices are indeed obtained, but the arrangement is now much less regular, particularly that of DFA. The mean dihedral angles, reported in Table 8, roughly correspond to α-helices, but the high standard deviations underline the structural irregularity. The heterogeneity of the DFA α-helix can be analyzed by plotting the (Φ/Ψ) sets along the sequence (Figure 5, red track). Not only do the ends of the chain deviate from the α-zone, but the middle of the chain fluctuates significantly within this zone. Both DFA and NMA chains have

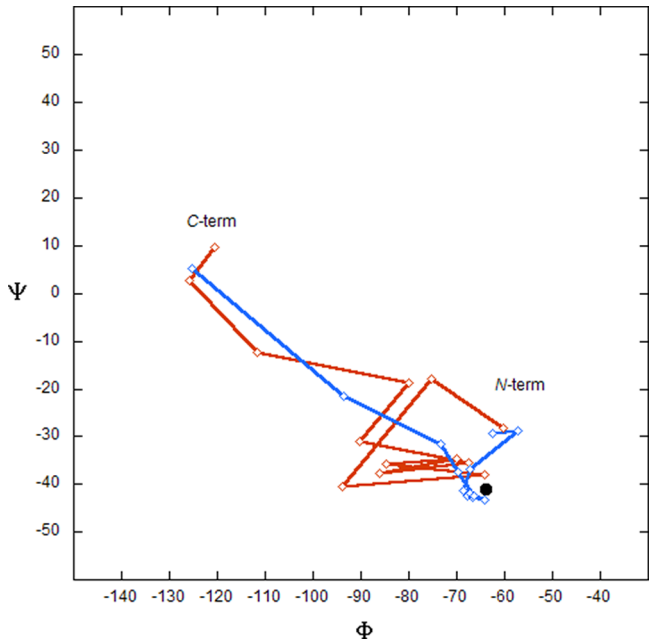

Figure 5. DFT-calculated (Φ/Ψ) sets along an α-helix built from 14 NMA (blue) or DFA (red) plaques. The isolated black dot marks the standard value found in protein α-helices (−64/41).

their *C*-terminal part in the δ-zone, but this affects more residues in DFA than in NMA.

In both cases, the expected hydrogen bonds are found, linking C=O (or B−F) of residue i to N−H of residue i + 4 (in terms of plaques, linking C=O (or B−F) of plaque i to N−H of plaque i + 3). Of the 11 possible such hydrogen bonds, only 10 are present in both cases, and the *C*-terminal parts have the structure of a δ or 3.10 helix, an end effect well-documented in peptide helical oligomers.[52] In both helices, the X−Y···H−N alignments are favorable, with mean distances of 2.04 Å for O···H and 2.32 Å for F···H and mean angles of 161° for O···H−N and 150° for F···H−N angles. Here again, standard deviations are larger in the DFA helix (0.10 Å, 11°) than in the NMA helix (0.06 Å, 5°). Because the B−F···H−N interaction is intrinsically less strong than the C=O···H−N one (see above), this should impart less stability to the DFA α-helix. In fact, its MPJE index is calculated at only −0.5 kcal/mol, the same value as that calculated in the δ helix (see Table 8), while that of NMA is of course much larger at −6 kcal/mol. In addition to the weakness of the F···H interaction, the DFA mean α-zone clearly falls within the δ catchment region (see Figure 3,

dx.doi.org/10.1021/jp304150p | J. Phys. Chem. B 2012, 116, 8863−8872

bottom), so that the α-helix and the δ-helix not only have comparable stability, but they should be easily converted into each other. In other words, some plasticity should here temper helical structuration.

CONCLUSIONS

In the quest of peptide-bond alternatives to be used in biological applications, the balance between geometrical structure similarities and chemical reactivity differences with respect to natural peptides acts as an essential guiding principle. The present work on model compounds has tried to assess, on structural grounds, how the properties of a natural peptide are affected by the simple replacement of the amide CO bond by a BF one. This replacement actually ensures a good isosterism, and because both atom pairs are strictly isoelectronic (4 + 6 = 3 + 7), it should basically preserve a similar electron organization. Nevertheless, enzyme extreme specificity should give rise to interesting differences in biochemical behavior, hence biological responses.

Substitution of a single amino acid residue by a DFA unit in a given protein would not turn down the two hydrogen bonds at this site, but with their strength being divided by a factor of 3 (or more), the whole secondary or tertiary structure should be somewhat altered, in particular in its flexibility properties. However, oligomers built from DFA plaques only, while exhibiting clear structuration, seem to show more plasticity than their peptide analogues.

Although further theoretical modeling is still required, for instance, on mixed systems in which both kinds of plaques abut on one another as in dipeptide models $CH_3-BF-NH-CH_2-CO-NH-CH_3$ or $CH_3-CO-NH-CH_2-BF-NH-CH_3$, the present preliminary study points to preservation of most of the salient feature of peptides. Whatever its use in peptidomimetics, biostability improvement, patching up, or scaffolding, and given the low toxicity of organoboron compounds, the −BF−NH− link therefore appears as a potentially promising peptide-bond surrogate.

AUTHOR INFORMATION

Corresponding Author

*E-mail: trinquier@irsamc.ups-tlse.fr.

Notes

The authors declare no competing financial interest.

ACKNOWLEDGMENTS

We thank Professor Colin Marsden for his help in improving the manuscript.

REFERENCES

(1) Hill, D. J.; Mio, M. J.; Prince, R. B.; Hughes, T. S.; Moore, J. S. *Chem. Rev.* **2001**, *101*, 3893−4011.
(2) Aleman, C. *J. Phys. Chem. A* **2001**, *105*, 6717−6723.
(3) Bursavich, M. G.; Rich, D. H. *J. Med. Chem.* **2002**, *45*, 541−558.
(4) Adessi, C.; Soto, C. *Curr. Med. Chem.* **2002**, *9*, 963−978.
(5) Perez, J. J.; Corcho, F.; Llorens, O. *Curr. Med. Chem.* **2002**, *9*, 2209−2229.
(6) Otvos, L., Jr. *Methods Mol. Biol.* **2008**, *494*, 1−8.
(7) Vagner, J.; Qu, H.; Hruby, V. J. *Curr. Opin. Chem. Biol.* **2008**, *12*, 292−296.
(8) Perez, J. J.; Corcho, F.; Rubio-Martinez, J. *Burger's Medicinal Chemistry, Drug Discovery, and Development*, 7th ed.; Abraham, D. J., Rotella, D. P., Eds.; John Wiley & Sons: New York, 2010; pp 1−44.
(9) Choudhary, A.; Raines, R. T. *ChemBioChem* **2011**, *12*, 1801−1807.
(10) Matteo, F.; Stefano, M. *Mol. Inf.* **2012**, *31*, 12−20.
(11) Abraham, L. J.; Ellison, S. L. R.; Schonholzer, P.; Thomas, W. A. *Tetrahedron* **1986**, *42*, 2101−2110.
(12) Van der Veken, P.; Senten, K.; Kertèsz, I.; de Meester, I.; Lambeir, A.-M.; Maes, M.-B.; Scharpé, S.; Haemers, A.; Augustyns, K. *J. Med. Chem.* **2005**, *48*, 1768−1780.
(13) Nakamura, Y.; Okada, M.; Koura, M.; Tojo, M.; Saito, A.; Sato, A.; Taguchi, T. *J. Fluorine Chem.* **2006**, *127*, 627−636.
(14) Urban, J. J.; Tillman, B. G.; Cronin, W. A. *J. Phys. Chem. A* **2006**, *110*, 11120−11129.
(15) Couve-Bonnaire, S.; Cahard, D.; Pannecoucke, X. *Org. Biomol. Chem.* **2007**, *5*, 1151−1157.
(16) Dutheuil, G.; Couve-Bonnaire, S.; Pannecoucke, X. *Angew. Chem., Int. Ed.* **2007**, *46*, 1290−1292.
(17) Couve-Bonnaire, S.; Cahard, D.; Pannecoucke, X. *Chim. Oggi* **2007**, *25* (suppl. 1), 30−32.
(18) Gorske, B. C.; Mbofana, C. T.; Miller, S. J. *Org. Lett.* **2009**, *11*, 4318−4321.
(19) McKinney, B. E.; Urban, J. J. *J. Phys. Chem. A* **2010**, *114*, 1123−1133.
(20) For statistic analysis of ω dihedral angles in proteins, see MacArthur, M. W.; Thornton, J. M. *J. Mol. Biol.* **1996**, *264*, 1180−1195.
(21) For BN/CC isosterism, see Liu, Z.; Marder, T. B. *Angew. Chem., Int. Ed.* **2008**, *47*, 242−244. Luo, W.; Zakharov, L. N.; Liu, S.-Y. *J. Am. Chem. Soc.* **2011**, *133*, 13006−13009.
(22) Burnham, B. S. *Curr. Med. Chem.* **2005**, *12*, 1995−2010.
(23) Malde, A. K.; Khedkar, S. A.; Coutinho, E. C. *Int. J. Quantum Chem.* **2005**, *102*, 734−742.
(24) Malde, A. K.; Khedkar, S. A.; Coutinho, E. C. *J. Chem. Theory Comput.* **2006**, *2*, 1664−1674.
(25) Malde, A. K.; Khedkar, S. A.; Coutinho, E. C. *J. Chem. Theory Comput.* **2006**, *2*, 312−321.
(26) Malde, A. K.; Khedkar, S. A.; Coutinho, E. C. *J. Chem. Theory Comput.* **2007**, *3*, 619−627.
(27) Malde, A. K.; Khedkar, S. A.; Coutinho, E. C. *J. Phys. Org. Chem.* **2007**, *20*, 151−160.
(28) Mo, Y.; Peyerimhoff, S. D. *Theor. Chem. Acc.* **1999**, *101*, 311−318.
(29) Frisch, M. J.; Trucks, G. W.; Schlegel, H. B.; Scuseria, G. E.; Robb, M. A.; Cheeseman, J. R.; Montgomery, J. A., Jr.; Vreven, T.; Kudin, K. N.; Burant, J. C.; Millam, J. M.; Iyengar, S. S.; Tomasi, J.; Barone, V.; Mennucci, B.; Cossi, M.; Scalmani, G.; Rega, N.; Petersson, G. A.; Nakatsuji, H.; Hada, M.; Ehara, M.; Toyota, K.; Fukuda, R.; Hasegawa, J.; Ishida, M.; Nakajima, T.; Honda, Y.; Kitao, O.; Nakai, H.; Klene, M.; Li, X.; Knox, J. E.; Hratchian, H. P.; Cross, J. B.; Bakken, V.; Adamo, C.; Jaramillo, J.; Gomperts, R.; Stratmann, R. E.; Yazyev, O.; Austin, A. J.; Cammi, R.; Pomelli, C.; Ochterski, J. W.; Ayala, P. Y.; Morokuma, K.; Voth, G. A.; Salvador, P.; Dannenberg, J. J.; Zakrzewski, V. G.; Dapprich, S.; Daniels, A. D.; Strain, M. C.; Farkas, O.; Malick, D. K.; Rabuck, A. D.; Raghavachari, K.; Foresman, J. B.; Ortiz, J. V.; Cui, Q.; Baboul, A. G.; Clifford, S.; Cioslowski, J.; Stefanov, B. B.; Liu, G.; Liashenko, A.; Piskorz, P.; Komaromi, I.; Martin, R. L.; Fox, D. J.; Keith, T.; Al-Laham, M. A.; Peng, C. Y.; Nanayakkara, A.; Challacombe, M.; Gill, P. M. W.; Johnson, B.; Chen, W.; Wong, M. W.; Gonzalez, C.; Pople, J. A. *Gaussian 03*, revision B.05; Gaussian, Inc.: Wallingford, CT, 2003.
(30) Vilani, V.; Alagona, G.; Ghio, C. *Mol. Eng.* **1999**, *8*, 135−153.
(31) Kang, Y. K. *J. Mol. Struct.* **2001**, *546*, 183−193.
(32) Mantz, Y. A.; Branduardi, D.; Bussi, G.; Parrinello, M. *J. Phys. Chem. B* **2009**, *113*, 12521−12529.
(33) The dipole moment of a peptide group is estimated at 3.5−3.7 D. In *trans*-NMA, it has been measured at 4.2 D: Rodrigo, M. M.; Tarazona, M. P.; Saiz, E. *J. Phys. Chem.* **1986**, *90*, 2236−2243. For systematic calculations of the dipole moment in *cis*- and *trans*-NMA at various theoretical levels, see ref 31.

(34) Wiberg, K. B.; Laidig, K. E. *J. Am. Chem. Soc.* **1987**, *109*, 5935−5943.
(35) Bharatam, P. V.; Moudgil, R.; Kaur, D. *J. Phys. Chem. A* **2003**, *107*, 1627−1634.
(36) Pimentel, G. C. *J. Chem. Phys.* **1951**, *19*, 446−448.
(37) Rundle, R. E. *J. Am. Chem. Soc.* **1963**, *85*, 112−113.
(38) Berski, S.; Latajka, Z.; Gordon, A. J. *New J. Chem.* **2011**, *35*, 89−96.
(39) Esposito, L.; De Simone, A.; Zagari, A.; Vitagliano, L. *J. Mol. Biol.* **2005**, *347*, 483−487.
(40) Mathieu, S.; Poteau, R.; Trinquier, G. *J. Phys. Chem. B* **2008**, *112*, 7894−7902.
(41) For a systematic study of the effect of heteroatom on the rotational barrier around C═C in substituted ethylenes, see Taddei, F. *J. Mol. Struct.: THEOCHEM* **2001**, *544*, 141−150.
(42) The double pathway also stands in unsubstituted 2-butene, where comparable barriers around 67 kcal/mol are also obtained at the same CASSCF(2,2) level of description.
(43) Mathieu, S.; Trinquier, G. *Phys. Chem. Chem. Phys.* **2009**, *11*, 8183−8190.
(44) At MP2 level, the planar pairing of *cis*-2FB dimer is not a true minimum on the potential energy surface but only a plateau point with weak energy gradient. Continuation of the optimization leads to hinge buckling into a nearly stacked form, hence the two blank cells in Table 5.
(45) The stretching force constant associated with each equivalent hydrogen bond is obtained straightforwardly from the relation

$$k = \frac{M}{4}\left\{\frac{\bar{\nu}}{1303}\right\}^2$$

in which k is expressed in mdyn/Å, M is the mass of the monomer, expressed in atomic mass units, and $\bar{\nu}$ is the wavenumber expressed in cm^{-1}.
(46) (a) Poteau, R.; Trinquier, G. *J. Am. Chem. Soc.* **2005**, *127*, 13875−13889. (b) Poteau, R.; Trinquier, G. *J. Org. Chem.* **2007**, *72*, 8251−8258.
(47) Strictly speaking, this is an inverse γ-turn, the most widespread, with mean dihedral set around (−79/69), while the regular γ-turn would correspond to symmetrical positions, with mean dihedral set at around (75/−64): Miner-White, E. J.; Ross, B. M.; Ismail, R.; Belhadj-Mostefa, K.; Poet, R. *J. Mol. Biol.* **1988**, *204*, 777−782. Miner-White, E. J. *J. Mol. Biol.* **1990**, *216*, 386. Guruprasad, K.; Rajkumar, S. *J. Biosci.* **2000**, *25*, 143−156.
(48) Note that such overlooking can be overcome by studying conformational maps of longer oligomers in which the same (Φ/Ψ) set is assigned to all Cα. Beyond a sufficient length, this allows the detection of all the possible helicoidal hydrogen bonding schemes.
(49) For glycine dipeptide theoretical Ramachandran maps, see, for instance, Fujitani, H.; Matsuura, A.; Sakai, S.; Sato, H.; Tanida, Y. *J. Chem. Theory Comput.* **2009**, *5*, 1155−1165. For glycine experimental Ramachandran maps, see Wathen, B.; Pratt, D. A.; Jia, Z. *ChemBioChem* **2011**, *12*, 1674−1677.
(50) We use here a convenient labelling proposed for *trans*-peptide maps: See Perczel, A.; Farkas, Ö.; Jakli, I.; Topol, I. A.; Csizmadia, I. G. *J. Comput. Chem.* **2003**, *24*, 1026−1042. Perczel, A.; Csizmadia, I. G. In *The Amide Linkage*; Greenberg, A., Breneman, C. M., Liebman, J. F., Eds.; Wiley-Interscience: New York, 2003; Chapter 13.
(51) (a) Law, J. M. S.; Setiadi, D. H.; Chass, G. A.; Csizmadia, I. G.; Viskolcz, B. *J. Phys. Chem. A* **2005**, *109*, 520−533. (b) Law, J. M. S.; Szori, M.; Izsak, R.; Penke, B.; Csizmadia, I. G.; Viskolcz, B. *J. Phys. Chem. A* **2006**, *110*, 6100−6111.
(52) (a) Petukhov, M.; Uegaki, K.; Yumoto, N.; Serrano, L. *Protein Sci.* **2002**, *11*, 766−777. (b) Ho, B. K.; Thomas, A.; Brasseur, R. *Protein Sci.* **2003**, *12*, 2508−2522.